

# Journal of Biomedical Optics

[SPIEDigitalLibrary.org/jbo](http://SPIEDigitalLibrary.org/jbo)

## **Detection of cerebral ischemia using the power spectrum of the pulse wave measured by near-infrared spectroscopy**

Akira Ebihara  
Yuichi Tanaka  
Takehiko Konno  
Shingo Kawasaki  
Michiyuki Fujiwara  
Eiju Watanabe

# Detection of cerebral ischemia using the power spectrum of the pulse wave measured by near-infrared spectroscopy

Akira Ebihara,<sup>a</sup> Yuichi Tanaka,<sup>a</sup> Takehiko Konno,<sup>b</sup> Shingo Kawasaki,<sup>c</sup> Michiyuki Fujiwara,<sup>c</sup> and Eiju Watanabe<sup>b</sup>

<sup>a</sup>Jichi Medical University, Saitama Medical Center, Department of Neurosurgery, 1-847 Amanuma-cho, Omiya-ku, Saitama-shi, Saitama 330-8503, Japan

<sup>b</sup>Jichi Medical University, Department of Neurosurgery, 3311-1 Yakushiji, Shimotsuke-shi, Tochigi 329-0498, Japan

<sup>c</sup>Hitachi Medical Corporation, 2-1 Shintoyohuta, Kashiwa-shi, Chiba 277-0804, Japan

**Abstract.** The diagnosis and medical treatment of cerebral ischemia are becoming more important due to the increase in the prevalence of cerebrovascular disease. However, conventional methods of evaluating cerebral perfusion have several drawbacks: they are invasive, require physical restraint, and the equipment is not portable, which makes repeated measurements at the bedside difficult. An alternative method is developed using near-infrared spectroscopy (NIRS). NIRS signals are measured at 44 positions (22 on each side) on the fronto-temporal areas in 20 patients with cerebral ischemia. In order to extract the pulse-wave component, the raw total hemoglobin data recorded from each position are band-pass filtered (0.8 to 2.0 Hz) and subjected to a fast Fourier transform to obtain the power spectrum of the pulse wave. The ischemic region is determined by single-photon emission computed tomography. The pulse-wave power in the ischemic region is compared with that in the symmetrical region on the contralateral side. In 17 cases (85%), the pulse-wave power on the ischemic side is significantly lower than that on the contralateral side, which indicates that the transmission of the pulse wave is attenuated in the region with reduced blood flow. Pulse-wave power might be useful as a noninvasive marker of cerebral ischemia. © The Authors. Published by SPIE under a Creative Commons Attribution 3.0 Unported License. Distribution or reproduction of this work in whole or in part requires full attribution of the original publication, including its DOI. [DOI: [10.1117/1.JBO.18.10.106001](https://doi.org/10.1117/1.JBO.18.10.106001)]

Keywords: near-infrared spectroscopy; cerebral ischemia; pulse wave; power spectrum.

Paper 130387RR received Jun. 4, 2013; revised manuscript received Aug. 23, 2013; accepted for publication Aug. 28, 2013; published online Oct. 1, 2013.

## 1 Introduction

Stroke is an important public health issue because it is a leading cause of death and disability. As a result of cerebral infarction, patients suffer severe disabilities such as consciousness disorder, paralysis, and aphasia. In the previous studies on the epidemiology of cerebral ischemia, risk factors such as hypertension, diabetes mellitus, and hypercholesterolemia were reported.<sup>1,2</sup> The number of patients with cerebral ischemia has been increasing recently, in accordance with an increase in patients with risk factors. Therefore, the diagnosis and medical treatment of cerebral ischemia are becoming increasingly important.

Assessment of cerebral perfusion is essential for the accurate diagnosis and medical treatment of patients with cerebral ischemia. In order to reduce permanent disability, the prevention and early detection of cerebral ischemia are very important. The development of a method for noninvasive and repeated measurement of cerebral perfusion is needed. Conventional methods for the evaluation of cerebral hemodynamics include cerebral catheter angiography,<sup>3,4</sup> computed tomography (CT),<sup>5,6</sup> magnetic resonance imaging (MRI),<sup>7-10</sup> transcranial Doppler (TCD),<sup>11,12</sup> single-photon emission computed tomography (SPECT),<sup>13,14</sup> and positron emission tomography (PET).<sup>15,16</sup> These techniques allow measurement of cerebral perfusion deficits, but they have several limitations. Cerebral catheter angiography is invasive, perfusion CT and MRI require injection

of a contrast agent, and SPECT and PET require administration of a radioisotope. Repeated measurement is often difficult because of these limitations. TCD and arterial spin-labeling MRI have been developed as noninvasive *in vivo* imaging methods. However, with TCD, the measurement area is limited, and the examination is dependent on the skill of the operator. Arterial spin-labeling MRI does not yet have sufficient diagnostic accuracy to be used in clinical practice. All of the aforementioned methods require restraint of the patient. Furthermore, measurements at the bedside cannot be performed, because the equipment required for these examinations (other than TCD) is not portable.

In contrast to these conventional methods, near-infrared spectroscopy (NIRS) can continuously measure real-time changes in the concentrations of oxygenated hemoglobin (Oxy-Hb), deoxygenated hemoglobin (Deoxy-Hb), and total hemoglobin (Total-Hb) in cerebral tissue.<sup>17-19</sup> Total-Hb is defined as the sum of Oxy-Hb and Deoxy-Hb. We focused on Total-Hb in this article, because changes in Total-Hb indicate changes in cerebral blood volume (CBV) and correlate with regional cerebral blood flow (CBF).<sup>20</sup> The basis of this approach is the modified Beer-Lambert law.<sup>21-23</sup> This method is suitable for repeated measurement of cerebral perfusion at the bedside, because it is simple, noninvasive, requires minimal patient restraint, has high-temporal resolution, and is portable.<sup>24,25</sup> NIRS has been increasingly used in recent years in various clinical fields including neurosurgery, neurology, psychiatry, and rehabilitation.<sup>26-29</sup> Although methods have been developed that use NIRS to measure cerebral perfusion,<sup>30-32</sup> these methods require improvement, because the measurements were

Address all correspondence to: Akira Ebihara, Jichi Medical University, Saitama Medical Center, Department of Neurosurgery, 1-847 Amanuma-cho, Omiya-ku, Saitama-shi, Saitama 330-8503, Japan. Tel: +81-48-647-2111; Fax: +81-48-644-8617; E-mail: [ebihara@jichi.ac.jp](mailto:ebihara@jichi.ac.jp)

performed using intravenous bolus injection of indocyanine green or oxygen inhalation.

Spontaneous oscillations associated with various physiological changes can be observed in the raw data measured by NIRS. Applying a fast Fourier transform (FFT) to the NIRS raw data results in peaks within specific frequency bands of the power spectrum such as the low-frequency oscillation band (<0.1 Hz), respiratory oscillation band (around 0.2 Hz), and cardiac oscillation band (around 1.0 Hz).<sup>33–37</sup> The cardiac oscillation was defined as the pulse wave. In a previous study, Voila et al. showed that the amplitude of the pulse wave was correlated with the changes in CBF in the middle cerebral artery (MCA) territory, and Kwan et al. reported a significant association between cortical perfusion and the pulse wave.<sup>38,39</sup>

The aim of this article was to develop a method for measuring cerebral perfusion using NIRS and to determine if pulse-wave power could serve as an index of cerebral ischemia. This technique has the potential to measure cerebral perfusion repeatedly and noninvasively at the bedside and does not suffer from the limitations of conventional methods that have been used to evaluate cerebral ischemia.

## 2 Subjects

Twenty patients with cerebral ischemia (16 men and 4 women; age range 59 to 77 years) participated in this study. In all subjects, a decrease in CBF in the MCA territory was observed on *N*-isopropyl-*p*-[<sup>123</sup>I] iodoamphetamine (<sup>123</sup>I-IMP)-SPECT imaging at rest. A stenosis or an occlusion of the internal carotid artery (ICA) or MCA was observed by cerebral catheter angiography or magnetic resonance angiography (MRA) in all cases, but cerebral infarction in the cerebral cortex of the MCA territory was not observed on MRI in any patient.

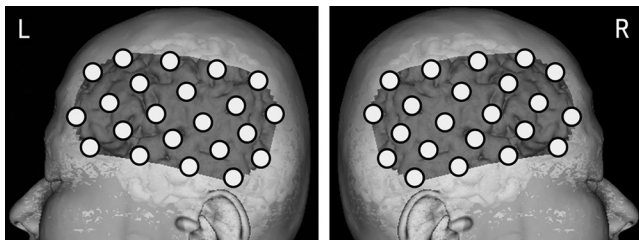


**Fig. 1** Configuration of the light probes. Measurement positions are shown. The light probes cover the bilateral fronto-temporal areas in order to measure the middle cerebral artery (MCA) territory.

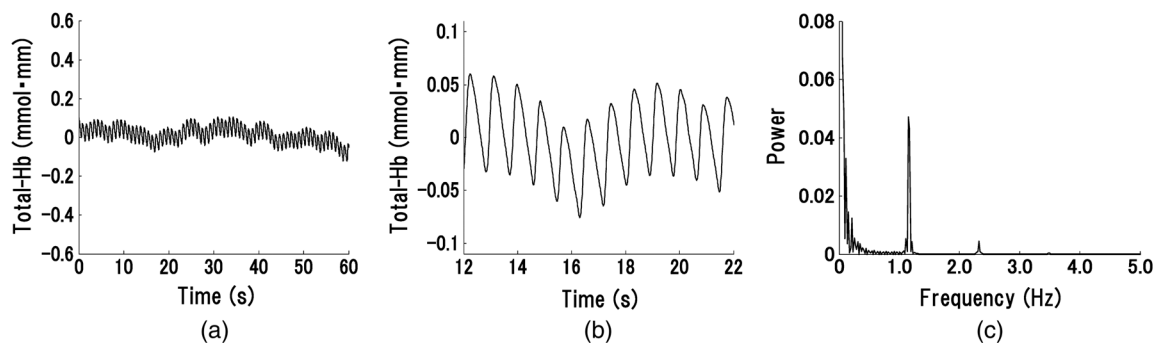


**Fig. 2** Waveform and power spectrum of the near-infrared spectroscopy (NIRS) signals. (a) Time course of raw Total-Hb data measured by NIRS in the resting state and (b) an enlarged view. (c) A fast Fourier transform (FFT) was applied to the Total-Hb data. The peak of the power spectrum is observed at the frequency band of the cardiac oscillation.

Furthermore, none of the patients had arrhythmias. The average duration from the detection of vascular lesions by cerebral catheter angiography or MRA to the time of NIRS measurement was 15 weeks.

This study was approved by the Ethics Committee of Jichi Medical University, and informed consent was obtained from all subjects.

## 3 Materials and Methods

### 3.1 Methods of Measurement for NIRS

Measurements were performed on a continuous-wave NIRS system (ETG-4000, Hitachi Medical Corporation, Tokyo, Japan) using two sets of  $3 \times 5$  probe arrays (each set had eight light-emitting sources and seven light detectors). In this system, near-infrared light rays with wavelengths of 695 and 830 nm were guided by optical fiber bundles and transmitted into the cranium. Reflections of the near-infrared rays were detected in receiving probes set on the scalp 30 mm away from the transmitting probes.<sup>40</sup> In order to measure the changes in concentrations of hemoglobin in the MCA territory, NIRS probes were symmetrically set on the subject's scalp to cover the bilateral fronto-temporal areas.<sup>32</sup> The NIRS signals were measured from 44 positions on the head (22 positions on each side). Measurement positions and covered areas are shown in Fig. 1. The sampling frequency used to extract the pulse-wave component was 10 Hz,<sup>35</sup> and each signal was recorded for 60 s. We were not able to obtain a stable waveform of the pulse wave when shorter measuring periods were used. On the other hand, with longer measuring periods, there were no differences in the stability of the pulse waveform. Since there were no advantages in measuring for shorter or longer periods, we recorded for 60 s to ensure a stable waveform. In order to minimize the influence of environmental factors on CBF, the subjects were seated comfortably and continued ordinary breathing during the measurement in a quiet room.

### 3.2 NIRS Data Analysis

The raw Total-Hb data [shown in Figs. 2(a) and 2(b)] measured by NIRS were analyzed by the following methods to investigate the changes in regional CBF associated with the cardiac oscillations. The NIRS data were processed using MATLAB R2011b (The MathWorks, Inc., Natick, Massachusetts).

Spectral analysis of the Total-Hb signal showed that the peak of the power spectrum associated with the cardiac oscillation was centered around 1.0 Hz, as shown in Fig. 2(c). In order to extract the pulse-wave component, the raw Total-Hb data recorded from each position were band-pass filtered (0.8 to 2.0 Hz) and subjected to FFT to obtain the power spectrum of the pulse wave. In each measuring position, the peak in the power spectrum that was due to the pulse wave was calculated. In all subjects, we confirmed that the peak of the power spectrum associated with cardiac oscillation was within this

frequency band. The peak in the power spectrum due to the pulse wave was defined as pulse-wave power. The reason for preprocessing the signals using the band-pass filter was to make it easier to confirm the waveform of the pulse wave. There was no difference between the pulse-wave power values determined with and without preprocessing using the band-pass filter. A contour map (topogram) was drawn using the pulse-wave power at each measuring position. In the topogram, the values between each measuring position were calculated by spline interpolation.

**Table 1** Clinical features and pulse-wave power data in patients with cerebral ischemia.

Case	Age	Sex	Vascular lesion	Ischemic side		Pulse-wave power		P-value
				SPECT	NIRS	Mean $\pm$ SD		
						L	R	
1	77	M	L ICA stenosis	L	L	0.073 $\pm$ 0.021	0.186 $\pm$ 0.096	0.011
2	61	M	L ICA stenosis	L	N	0.135 $\pm$ 0.049	0.181 $\pm$ 0.064	0.058
3	78	M	L ICA stenosis	L	L	0.022 $\pm$ 0.011	0.045 $\pm$ 0.024	0.038
4	75	M	R ICA stenosis	R	R	0.042 $\pm$ 0.012	0.019 $\pm$ 0.009	0.004
5	67	M	R ICA stenosis	R	R	0.152 $\pm$ 0.052	0.067 $\pm$ 0.047	0.007
6	60	M	R ICA stenosis	R	R	0.139 $\pm$ 0.059	0.061 $\pm$ 0.038	0.007
7	77	M	L ICA stenosis	L	L	0.039 $\pm$ 0.019	0.251 $\pm$ 0.296	0.0002
8	65	M	R ICA stenosis	R	R	0.054 $\pm$ 0.009	0.013 $\pm$ 0.008	0.016
9	63	M	R ICA stenosis	R	R	0.115 $\pm$ 0.034	0.071 $\pm$ 0.028	0.017
10	77	M	L ICA stenosis	L	L	0.018 $\pm$ 0.015	0.058 $\pm$ 0.026	0.0006
11	70	F	L ICA stenosis	L	L	0.028 $\pm$ 0.004	0.066 $\pm$ 0.045	0.017
12	65	M	R ICA occlusion	R	R	0.083 $\pm$ 0.084	0.019 $\pm$ 0.013	0.038
13	74	F	R ICA stenosis	R	N	0.062 $\pm$ 0.036	0.045 $\pm$ 0.032	0.097
14-1	65	F	L ICA stenosis	L	L	0.014 $\pm$ 0.004	0.037 $\pm$ 0.027	0.008
14-2	65	F	After CAS	N	N	0.027 $\pm$ 0.015	0.034 $\pm$ 0.011	0.548
15-1	71	M	L ICA stenosis	L	L	0.027 $\pm$ 0.014	0.116 $\pm$ 0.023	0.0002
15-2	71	M	After CAS	N	N	0.182 $\pm$ 0.081	0.146 $\pm$ 0.058	0.373
16	66	M	R MCA stenosis	R	N	0.059 $\pm$ 0.029	0.028 $\pm$ 0.012	0.095
17	67	M	L ICA stenosis	L	L	0.023 $\pm$ 0.014	0.052 $\pm$ 0.023	0.006
18	59	M	L ICA occlusion	L	L	0.098 $\pm$ 0.056	0.246 $\pm$ 0.191	0.003
19	66	M	R MCA stenosis	R	R	0.069 $\pm$ 0.021	0.032 $\pm$ 0.014	0.0001
20	62	F	L ICA stenosis	L	L	0.058 $\pm$ 0.026	0.177 $\pm$ 0.099	0.009

R: right, L: left, N: no significant difference.

MCA: middle cerebral artery.

ICA: internal carotid artery.

SPECT: single-photon emission computed tomography.

NIRS: near-infrared spectroscopy.

CAS: carotid artery stenting.

Cerebral ischemic side determined by  $^{123}\text{I}$ -IMP-SPECT and NIRS and the mean  $\pm$  one standard deviation of pulse-wave power measured by NIRS and *P*-values of Mann-Whitney *U* test are shown in the columns. *P*-values are for the difference between the R and L sides.

### 3.3 Evaluation of Cerebral Ischemia

$^{123}\text{I}$ -IMP-SPECT was used to define the ischemic region. The ipsilateral region that had  $<90\%$  of the counts obtained on the contralateral side was defined as the ischemic region. No attempt was made to define the precise borders of the ischemic region. Thus, we evaluated the pulse-wave power from NIRS channels both within and outside the ischemic region. The mean of all pulse-wave power values on the ipsilateral side was compared with the mean of all pulse-wave power values from symmetrical recording sites on the contralateral side.

A Shapiro–Wilk normality test was performed to determine whether the pulse-wave power values were normally distributed. Since not all of the pulse-wave power values had a normal distribution in each patient, the pulse-wave power values were compared between the ipsilateral and the contralateral sides using nonparametric methods. The pulse-wave power values from the two sides in each patient were treated as unpaired groups, and the mean pulse-wave power was compared between the two groups using a Mann–Whitney  $U$  test. Differences with  $P < 0.05$  were considered significant.

## 4 Results

The mean pulse-wave power obtained from all of the NIRS channels on the ipsilateral side that included the ischemic region, as defined by  $^{123}\text{I}$ -IMP-SPECT, was significantly lower as compared with the contralateral side. Furthermore, the general location of the ischemic region could also be detected in the topogram of pulse-wave power, and this region was consistent with the ischemic region shown on  $^{123}\text{I}$ -IMP-SPECT. Results of all cases of cerebral ischemia are shown in Table 1. The cerebral ischemic side determined by  $^{123}\text{I}$ -IMP-SPECT and the mean of pulse-wave power measured by NIRS are shown in this table. In all cases, the side of lower pulse-wave power was consistent with the ischemic side as defined by  $^{123}\text{I}$ -IMP-SPECT, and there were significant

differences in the pulse-wave power between the two sides in 17 patients (85%). Moreover, in two patients (Table 1: cases 14 and 15), who underwent carotid artery stenting (CAS), the NIRS findings were compared with those of  $^{123}\text{I}$ -IMP-SPECT imaging. After CAS, increase in CBF in the ischemic region were observed by both  $^{123}\text{I}$ -IMP-SPECT and pulse-wave power. Significant differences in the mean of pulse-wave power between the two sides were not observed after CAS, as shown in Table 1. When the power spectrum of the pulse wave was determined using either the Oxy-Hb or Deoxy-Hb data, the detection rate of cerebral ischemia was inferior compared with Total-Hb.

### 4.1 Typical Case of Cerebral Ischemia (Table 1: Case 14)

A 65-year-old female patient had severe stenosis in the left cervical ICA that was observed by angiogram [Fig. 3(a)]. A decrease in CBF in the left cerebral hemisphere was observed on  $^{123}\text{I}$ -IMP-SPECT imaging [Fig. 3(b)]. CAS was performed in the left cervical ICA [Fig. 3(c)]. An increase in CBF in the left cerebral hemisphere was observed on  $^{123}\text{I}$ -IMP-SPECT imaging after CAS [Fig. 3(d)]. Before CAS, the amplitude and the power of the pulse-wave NIRS signals were lower in the ischemic region than those in the contralateral normal region (Fig. 4). This could be seen in the topogram of pulse-wave power [Fig. 5(a)]. The mean pulse-wave power on the ipsilateral side that included the ischemic region was 0.014 compared with 0.037 on the contralateral side (Table 1: case 14-1), and the difference was significant ( $P = 0.008$ , Mann–Whitney  $U$  test). After CAS, the pulse-wave power from a single channel in the ischemic region was increased compared with that seen before CAS (Fig. 6). These findings were confirmed in the topogram [Fig. 5(b)]. The mean of pulse-wave power on the ipsilateral side that included the ischemic region after CAS was 0.027 compared with 0.034 on the contralateral side

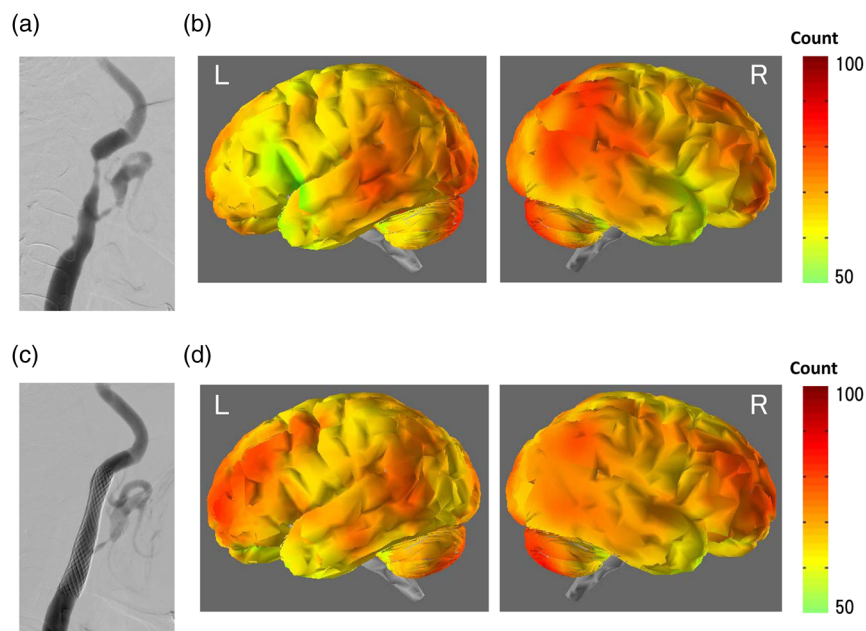


**Fig. 3** Angiogram and  $N$ -isopropyl- $p$ - $^{123}\text{I}$  iodoamphetamine ( $^{123}\text{I}$ -IMP)-SPECT images before and after carotid artery stenting (CAS). (a) Angiogram shows severe stenosis of the left cervical internal carotid artery (ICA). (b)  $^{123}\text{I}$ -IMP-SPECT demonstrates a decrease in cerebral blood flow (CBF) in the left MCA territory before CAS. (c) The ICA was dilated by CAS. (d)  $^{123}\text{I}$ -IMP-SPECT demonstrates an increase in CBF in the left MCA territory caused by CAS.

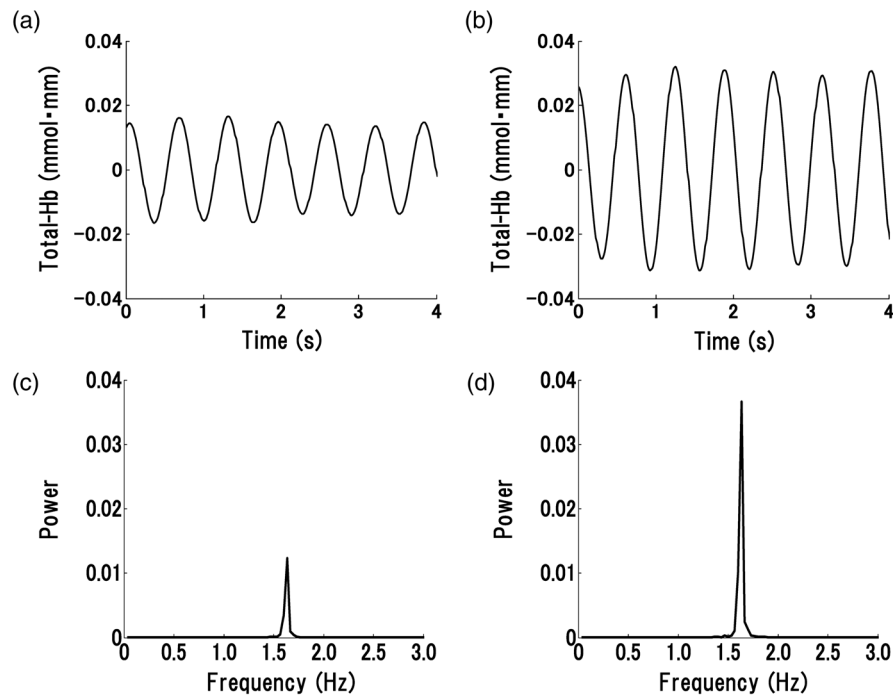


**Fig. 4** Waveforms and power spectra of the pulse wave (before CAS). (a) Waveforms of pulse wave in the ischemic region and (b) in the contralateral region. (c) Power spectra of pulse wave in the ischemic region and (d) in the contralateral region. The peak in power spectrum of the pulse wave is defined as pulse-wave power.

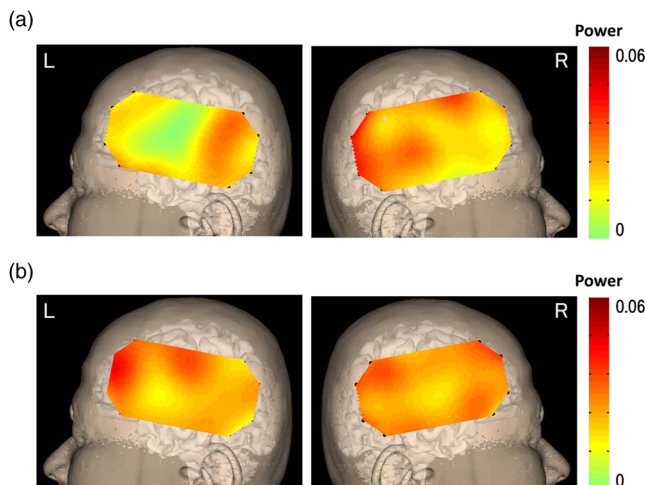


**Fig. 5** Topogram of pulse-wave power before and after CAS. (a) Lower pulse-wave power in the ischemic region compared with the contralateral region is shown in the topogram before CAS. (b) An increase in pulse-wave power in the ischemic region is shown in the topogram after CAS.

(Table 1: case 14-2), and the difference was not significant ( $P = 0.548$ , Mann-Whitney  $U$  test). These findings were consistent with the  $^{123}\text{I}$ -IMP-SPECT findings.

Figure 7 shows the mean pulse-wave power on the side with cerebral ischemia plotted against the mean pulse-wave power on the contralateral side in all patients with cerebral ischemia.

## 5 Discussion

Measurement data using NIRS show complex changes in hemoglobin by various physiological factors such as blood pressure,

respiration, and brain activity. Information from the pulse wave associated with cardiac oscillations could be obtained by investigating the changes in Total-Hb. Oscillations in the pulse wave measured by NIRS were often considered to be noise and eliminated by filtering. However, advanced signal-processing techniques applied to these oscillations can extract important information about cerebral perfusion. The present study showed that pulse-wave power was lower on the ipsilateral side that included the ischemic region compared with the normal region on the contralateral side. We could not measure the relative change in CBV due to cerebral ischemia, because we had no preischemic NIRS recordings. However, we substituted the NIRS measurements on the nonischemic contralateral side for a baseline, since symmetrical regions on the two hemispheres should have similar pulse-wave power values in the absence of ischemia. Thus, all the measurements on the ipsilateral side were compared with the values on the contralateral side. In all cases of cerebral ischemia, the side with lower pulse-wave power was consistently the ischemic side, as determined by  $^{123}\text{I}$ -IMP-SPECT imaging, and significant differences were obtained in 17 of 20 cases. In the cases without significant differences, only a slight CBF reduction was observed on the  $^{123}\text{I}$ -IMP-SPECT images. Differences in pulse-wave power were not significant between the two sides, because the decrease in the pulse wave amplitude were small in cases of mild ischemia. Therefore, it was thought that detection of mild ischemia was difficult with the present method. In order to improve the detection accuracy of cerebral ischemia, it will be important to determine the correlation between the decrease in pulse-wave power and the degree of reduction in CBF in different regions.

The findings of  $^{123}\text{I}$ -IMP-SPECT imaging were compared before and after CAS in two patients in our study. In the regions where CBF was lower than the normal regions before CAS, an increase in CBF was only observed on the ipsilateral side after

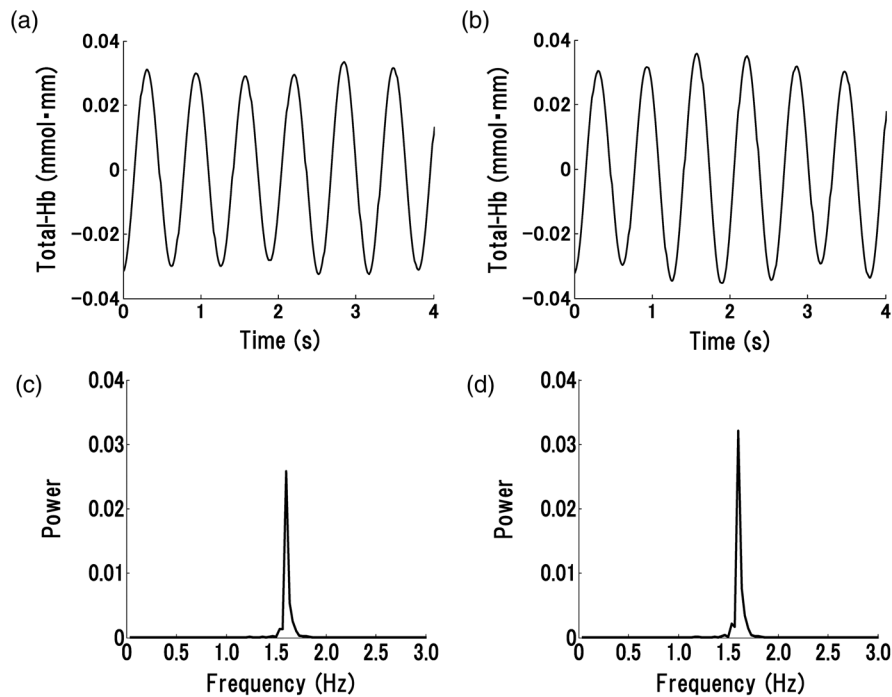


**Fig. 6** Waveforms and power spectra of pulse wave (after CAS). (a) Waveforms of the pulse wave in the ischemic region and (b) in the contralateral region. (c) Power spectra of the pulse wave in the ischemic region and (d) in the contralateral region.

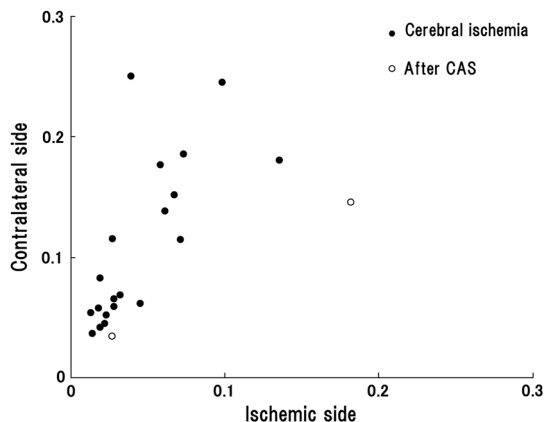


**Fig. 7** Scatter plot of the mean pulse-wave power. The x-axis shows the mean of pulse-wave power on the ischemic side as defined by  $^{123}\text{I}$ -IMP-SPECT. The y-axis shows the mean of pulse-wave power on the contralateral side. The results of cerebral ischemia are represented by closed circles, and the results after CAS are represented by open circles.

CAS. In these cases, the pulse-wave power measured by NIRS increased after CAS in the regions where it had been lower than normal before CAS. Increases in the pulse-wave power were consistent with improvements of CBF detected by  $^{123}\text{I}$ -IMP-SPECT imaging. Arterial pulsation is caused by cardiac systole, and the pressure pulse is transmitted throughout the arterial network, which results in local expansion of the elastic arterial walls. These local expansions of the arteries cause an increase in light absorption due to an increase in blood volume and consequently a decrease in the light intensity measured by NIRS.<sup>38,41</sup> In the ischemic region, the local arterial expansion might be reduced due to the attenuation of arterial pressure caused by a decrease in CBF. Therefore, the pulse-wave

power decreased, because the pulse wave oscillations are reduced compared with the normal region. Furthermore, the pulse-wave power increased after CAS, because the transmission of the pulse wave was restored by CAS.

It is important to note that there was an unavoidable influence of blood flow to the scalp on pulse-wave power, because the concentration of hemoglobin is measured through the scalp with the NIRS system. A previous study reported that the NIRS system could measure pulse waves that reflected changes in Total-Hb in cerebral tissue associated with the cardiac oscillation, and the amplitude and the power of pulse wave were correlated with changes in CBF.<sup>38,39</sup> Moreover, the change in pulse wave amplitude in the MCA territory was highly correlated with the change in CBF measured by TCD.<sup>38</sup> In the present study, the improvement of blood flow that followed CAS in two cases was observed mainly in the region of the ICA, and there was little effect on blood flow in the region of the external carotid artery. Therefore, we believe that a change in blood flow through the ICA was mainly responsible for the change in pulse-wave power.

In addition, measurement of continuous-wave NIRS is dependent on the modified Beer-Lambert law and includes optical path length as a component in the measured data. The optical path length is known to differ across different head regions. An unknown optical path length was a problem in the analysis of the data, because the true optical path length is difficult to measure by a continuous-wave NIRS system. The spatial variance on one side of the head may include variation due to differences in the optical path length as well as variation due to differences in CBF. Since no attempt was made to define the precise ischemic zone borders, we were not able to correlate the  $^{123}\text{I}$ -IMP-SPECT images from different local regions with their corresponding NIRS values recorded on the surface of the head. Also, we do not know the precise brain area registered by each different NIRS channel. However, a previous

study showed that the optical path lengths were similar among nearby channels and between homologous regions of the left and right hemispheres within a subject.<sup>42</sup> Asymmetry in cerebral hemodynamics between hemispheres due to cardiac oscillations could be detected by continuous-wave NIRS.<sup>43</sup> We compared the mean pulse-wave power on the ipsilateral side that included the ischemic region with the mean pulse-wave power from a symmetrical region on the contralateral side of the head. This was done to reduce the influence of differences in optical path lengths at different recording sites. We could not absolutely classify the pulse-wave power recorded in each channel as ischemic or nonischemic. However, the general location of the lower pulse-wave power was similar to the ischemic region defined by <sup>123</sup>I-IMP-SPECT imaging. Therefore, we could detect the presence of cerebral ischemia and the general location of the ischemic region using this method.

## 6 Conclusions

A method of using the power spectrum of the pulse wave measured by NIRS was developed to detect cerebral ischemia. It appeared that pulse-wave power could be a useful index of cerebral ischemia. The present method was clinically useful because we could detect cerebral ischemia repeatedly and non-invasively at the bedside.

## References

- M. Murat Sumer and O. Erturk, "Ischemic stroke subtypes: risk factors, functional outcome and recurrence," *Neurol. Sci.* **22**(6), 449–454 (2002).
- A. J. Grau et al., "Risk factors, outcome, and treatment in subtypes of ischemic stroke: the German stroke data bank," *Stroke* **32**(11), 2559–2566 (2001).
- M. Komiyama et al., "Prospective analysis of complications of catheter cerebral angiography in the digital subtraction angiography and magnetic resonance era," *Neurol. Med. Chir.* **38**(9), 534–540 (1998).
- T. J. Kaufmann et al., "Complications of diagnostic cerebral angiography: evaluation of 19,826 consecutive patients," *Radiology* **243**(3), 812–819 (2007).
- M. Wintermark et al., "Accuracy of dynamic perfusion CT with deconvolution in detecting acute hemispheric stroke," *AJNR Am. J. Neuroradiol.* **26**(1), 104–112 (2005).
- M. W. Parsons, "Perfusion CT: is it clinically useful?," *Int. J. Stroke* **3**(1), 41–50 (2008).
- L. Ostergaard et al., "Absolute cerebral blood flow and blood volume measured by magnetic resonance imaging bolus tracking: comparison with positron emission tomography values," *J. Cereb. Blood Flow Metab.* **18**(4), 425–432 (1998).
- H. Endo et al., "Quantitative assessment of cerebral hemodynamics using perfusion-weighted MRI in patients with major cerebral artery occlusive disease: comparison with positron emission tomography," *Stroke* **37**(2), 388–392 (2006).
- Y. Uchihashi et al., "Clinical application of arterial spin-labeling MR imaging in patients with carotid stenosis: quantitative comparative study with single-photon emission CT," *AJNR Am. J. Neuroradiol.* **32**(8), 1545–1551 (2011).
- B. Wu et al., "Collateral circulation imaging: MR perfusion territory arterial spin-labeling at 3T," *AJNR Am. J. Neuroradiol.* **29**(10), 1855–1860 (2008).
- A. M. Demchuk et al., "Specific transcranial Doppler flow findings related to the presence and site of arterial occlusion," *Stroke* **31**(1), 140–146 (2000).
- Y. You et al., "Detection of the siphon internal carotid artery stenosis: transcranial Doppler versus digital subtraction angiography," *J. Neuroimaging* **20**(3), 234–239 (2010).
- W. H. Knapp, R. von Kummer, and W. Kübler, "Imaging of cerebral blood flow-to-volume distribution using SPECT," *J. Nucl. Med.* **27**(4), 465–470 (1986).
- I. Podreka et al., "Quantification of regional cerebral blood flow with IMP-SPECT. Reproducibility and clinical relevance of flow values," *Stroke* **20**(2), 183–191 (1989).
- R. A. Koeppe et al., "Examination of assumptions for local cerebral blood flow studies in PET," *J. Nucl. Med.* **28**(11), 1695–1703 (1987).
- J. H. Greenberg et al., "Validation studies of iodine-123-iodoamphetamine as a cerebral blood flow tracer using emission tomography," *J. Nucl. Med.* **31**(8), 1364–1369 (1990).
- F. F. Jöbbsis, "Noninvasive, infrared monitoring of cerebral and myocardial oxygen sufficiency and circulatory parameters," *Science* **198**(4323), 1264–1267 (1977).
- T. Yamamoto et al., "Development and application of noninvasive optical topography," *Proc. SPIE* **4082**, 24–33 (2000).
- E. M. Hillman, "Optical brain imaging in vivo: techniques and applications from animal to man," *J. Biomed. Opt.* **12**(5), 051402 (2007).
- W. Lichty, K. Sakatania, and H. Zou, "Application of near-infrared spectroscopy to investigate brain activity: clinical research," *Proc. SPIE* **4082**, 34–39 (2000).
- A. Villinger and B. Chance, "Non-invasive optical spectroscopy and imaging of human brain function," *Trends Neurosci.* **20**(10), 435–442 (1997).
- M. Cope et al., "Methods of quantitating cerebral near infrared spectroscopy data," *Adv. Exp. Med. Biol.* **222**, 183–189 (1988).
- A. Maki et al., "Spatial and temporal analysis of human motor activity using noninvasive NIR topography," *Med. Phys.* **22**(12), 1997–2005 (1995).
- E. Watanabe et al., "Non-invasive functional mapping with multi-channel near infra-red spectroscopic topography in humans," *Neurosci. Lett.* **205**(1), 41–44 (1996).
- K. Isobe et al., "Functional imaging of the brain in sedated newborn infants using near infrared topography during passive knee movement," *Neurosci. Lett.* **299**(3), 221–224 (2001).
- E. Watanabe et al., "Noninvasive cerebral blood volume measurement during seizures using multichannel near infrared spectroscopic topography," *J. Biomed. Opt.* **5**(3), 287–290 (2000).
- R. P. Kannan et al., "Non-invasive assessment of language lateralization by transcranial near infrared optical topography and functional MRI," *Hum. Brain Mapp.* **16**(3), 183–189 (2002).
- K. Matsuo et al., "Alteration of hemoglobin oxygenation in the frontal region in elderly depressed patients as measured by near-infrared spectroscopy," *J. Neuropsychiatry Clin. Neurosci.* **12**(4), 465–471 (2000).
- P. M. Arendt, J. H. Ricker, and M. T. Schultheis, "Applications of functional near-infrared spectroscopy (fNIRS) to neurorehabilitation of cognitive disabilities," *Clin. Neuropsychol.* **21**(1), 38–57 (2007).
- W. M. Kuebler et al., "Noninvasive measurement of regional cerebral blood flow by near-infrared spectroscopy and indocyanine green," *J. Cereb. Blood Flow Metab.* **18**(4), 445–456 (1998).
- C. Terborg et al., "Bedside assessment of cerebral perfusion reductions in patients with acute ischemic stroke by near-infrared spectroscopy and indocyanine green," *J. Neurol. Neurosurg. Psychiatry* **75**(1), 38–42 (2004).
- A. Ebihara et al., "Evaluation of cerebral ischemia using near-infrared spectroscopy with oxygen inhalation," *J. Biomed. Opt.* **17**(9), 96002 (2012).
- C. E. Elwell et al., "Oscillations in cerebral haemodynamics. Implications for functional activation studies," *Adv. Exp. Med. Biol.* **471**, 57–65 (1999).
- H. Obrig et al., "Spontaneous low frequency oscillations of cerebral hemodynamics and metabolism in human adults," *Neuroimage* **12**(6), 623–639 (2000).
- T. Katura et al., "Quantitative evaluation of interrelations between spontaneous low-frequency oscillations in cerebral hemodynamics and systemic cardiovascular dynamics," *Neuroimage* **31**(4), 1592–1600 (2006).
- Y. Tong and B. D. Frederick, "Time lag dependent multimodal processing of concurrent fMRI and near-infrared spectroscopy (NIRS) data suggests a global circulatory origin for low-frequency oscillation signals in human brain," *Neuroimage* **53**(2), 553–564 (2010).
- Y. Tong, K. P. Lindsey, and B. de Frederick, "Partitioning of physiological noise signals in the brain with concurrent near-infrared

- spectroscopy and fMRI," *J. Cereb. Blood Flow Metab.* **31**(12), 2352–2362 (2011).
38. S. Viola et al., "Correlation between the arterial pulse wave of the cerebral microcirculation and CBF during breath holding and hyperventilation in human," *Clin. Neurophysiol.* **123**(10), 1931–1936 (2012).
  39. H. C. Kwan et al., "Human cortical perfusion and the arterial pulse: a near-infrared spectroscopy study," *BMC Physiol.* **4**(7) (2004).
  40. H. Sato et al., "Practicality of wavelength selection to improve signal-to-noise ratio in near-infrared spectroscopy," *Neuroimage* **21**(4), 1554–1562 (2004).
  41. G. Themelis et al., "Near-infrared spectroscopy measurement of the pulsatile component of cerebral blood flow and volume from arterial oscillations," *J. Biomed. Opt.* **12**(1), 014033 (2007).
  42. A. Katagiri et al., "Mapping of optical pathlength of human adult head at multi-wavelengths in near infrared spectroscopy," *Adv. Exp. Med. Biol.* **662**, 205–212 (2010).
  43. S. Muehlschlege et al., "Feasibility of NIRS in the neurointensive care unit: a pilot study in stroke using physiological oscillations," *Neurocrit. Care* **11**(2), 288–295 (2009).